

Review

Instant Attraction: Clay Authigenesis in Fossil Fungal Biofilms

Therese Sallstedt ^{1,*}, Magnus Ivarsson ^{1,2}, Henrik Drake ³ and Henrik Skogby ⁴

¹ Department of Paleobiology, Swedish Museum of Natural History, 11418 Stockholm, Sweden

² Department of Biology, University of Southern Denmark, Campusvej 55, Odense M, 5230 Odense, Denmark

³ Department of Biology and Environmental Science, Linnaeus University, 39182 Kalmar, Sweden

⁴ Department of Geology, Swedish Museum of Natural History, 11418 Stockholm, Sweden

* Correspondence: therese.sallstedt@nrm.se

Received: 25 June 2019; Accepted: 21 August 2019; Published: 24 August 2019



Abstract: Clay authigenesis associated with the activity of microorganisms is an important process for biofilm preservation and may provide clues to the formation of biominerals on the ancient Earth. Fossilization of fungal biofilms attached to vesicles or cracks in igneous rock, is characterized by fungal-induced clay mineralization and can be tracked in deep rock and deep time, from late Paleoproterozoic (2.4 Ga), to the present. Here we briefly review the current data on clay mineralization by fossil fungal biofilms from oceanic and continental subsurface igneous rock. The aim of this study was to compare the nature of subsurface fungal clays from different igneous settings to evaluate the importance of host rock and ambient redox conditions for clay speciation related to fossil microorganisms. Our study suggests that the most common type of authigenic clay associated with pristine fossil fungal biofilms in both oxic (basaltic) and anoxic (granitic) settings are montmorillonite-like smectites and confirms a significant role of fungal biofilms in the cycling of elements between host rock, ocean and secondary precipitates. The presence of life in the deep subsurface may thus prove more significant than host rock geochemistry in directing the precipitation of authigenic clays in the igneous crust, the extent of which remains to be fully understood.

Keywords: clay authigenesis; fossil fungi; igneous crust; cryptoendoliths; seafloor habitats

1. Introduction

The formation of authigenic minerals is a fundamental aspect of the interaction between microbial life and the ambient environment [1–10]. Throughout major parts of Earth history, clay minerals and low-crystalline amorphous aluminosilicate-phases dominated by a Fe-Al-Si composition, have been associated with biology, often in the form of clay mineralized prokaryotic [4,5,7,11,12] or eukaryotic cells and biofilms [13–19]. The close association and interconnection between microbes and authigenic clays have been demonstrated in vitro from laboratory culture experiments [20,21], but also from natural sedimentary environments, lacustrine sediments [2,4,5,22], hydrothermal areas [23], terrestrial rock habitats [24] and within the subsurface igneous biosphere of both continents and oceans [15–18,25]. Over the past decade, several studies have emphasized the importance of a subsurface crustal biota and its prominent role in element cycling, rock weathering and precipitation of secondary minerals [15–19,25–28]. Because of the vastness and relative inaccessibility of the deep biosphere in the oceanic and continental crust, however, more work is needed in order to fully comprehend and characterize the specific nature of life and trophic systems in the subsurface crust.

The current knowledge of deep biosphere-ecology is primarily based on traces of presumed microbial activity within the glassy rim of basaltic rocks [29–31], as well as body fossils within seafloor igneous settings [13–19,25,32–39]. In particular, fungal filaments and biofilms preserved by

authigenic clays seems to represent a large fraction of the deep biosphere fossil biotas [16–19,33–36,38]. While the presence of fossil fungi from the oceanic crust have been well established during the last decade, new research confirms a significant fungal presence also within the anoxic continental crust [25,39,40]. In drill cores from the Laxemar site, near Äspö hard rock laboratory in Sweden, partly carbonaceous and clay mineralized fungi have been identified within a granite hosted vein-system, associated with reducing minerals such as pyrite, which indicates that the granite-dwelling fungal communities had a largely anaerobic lifestyle [25].

The mode of clay encrustation within microorganisms in deep subsurface habitats resembles that identified within bacteria and prokaryotic biofilms in lake sediments, previously described by Ferris et al. [1,3], Konhauser and Urrutia [7] and Konhauser et al. [12], among others. This similarity not only suggests a common genesis, but, more importantly, highlights the affinity of microbial cells and their extracellular polymeric substances (EPS) to attract clay-forming elements leading to the formation of authigenic minerals. An important characteristic, therefore, of all cellular surfaces and their EPS, is the high reactivity and potential to adsorb, retain and exchange chemical species, including elements essential for microbial metabolism [41,42]. These characteristics can lower activation-energy and thus invoke nucleation of secondary minerals in association with microbial walls or sheaths [8,43–47]. This is also true of phyllosilicate minerals per se, and both clays and the reactive cell or biofilm surfaces, can therefore be considered important targets for understanding biogeochemical element cycling and the transfer of elements between rock, hydrosphere and the biota [48].

Most previous studies concerning microbial clay mineralization have focused on the role of prokaryotic microorganisms in shallow settings, such as soils, riverine, ocean and geothermal-sediments, as well as terrestrial flood basalts [1,2,4,5,11,23]. However, the increased understanding and characterization of extreme oligotrophic habitats in igneous rock calls for a closer examination of clay authigenesis within the subsurface crust. Understanding fossilization processes and the timing and mode of microbial preservation, can give important clues to the nature of life and its interaction with the environment. Therefore, the overall aim of this study is to add insight into the unexplored subject of fungal clay fossilization, by comparing the geochemistry of fungal clay precipitates from various igneous subsurface localities. New X-ray powder diffraction (XRD) and Mössbauer Spectroscopy data from Pacific Ocean pillow basalt and two anoxic fractured granite cores from Laxemar, Sweden, was added in order to determine and compare clay chemistry and Fe oxidation states between anoxic and oxic settings.

Our review suggests that intrinsic factors such as the structure of fungal biofilms may have a larger effect on the mineralogy of fungal clays compared to abiotically precipitated clays forming solely in equilibrium with surrounding source rock and fluids.

2. Methods

2.1. X-Ray Powder Diffraction

We used X-ray powder diffraction in order to analyse the mineralogical composition of authigenic clays from subsurface anoxic granite rocks and oxygenated basaltic seafloor rocks. The samples were removed from different depths and carefully extracted from split drill-cores using sterile forceps. The first sample consisted entirely of fungal filaments from a well-preserved biofilm (granite sample XLX09). A second, darker, clay phase represented a less well-preserved biofilm matrix (granite sample XCX04). A third clay sample (basalt sample 1205A-024R) associated with fungal filaments was scraped from a split drill core originating from the Pacific Ocean Nintoku seamount. The XRD patterns were collected using a Panalytical X'pert powder diffractometer (PANalytical B.V., Almelo, The Netherlands) equipped with an X'celerator silicon-strip detector. The range 5–80° (2 θ) was scanned with a step-size of 0.017° using a sample spinner with finely ground sample material mounted on a background-free silicon holder. All samples were mixed with dH₂O and run a second time, to evaluate the potential effect of clay swelling on the XRD spectra.

2.2. Mössbauer Spectroscopy

To characterize the redox state of Fe within the three clay samples investigated with XRD described above, Mössbauer spectra were measured on samples XLX09 (anoxic granite), XCX04 (anoxic granite) and 1205A-024R (oxic Pacific Ocean basalt) using a conventional spectrometer system operated in constant-acceleration mode. Due to limited amounts of sample material, a ^{57}Co rhodium matrix point-source with a nominal activity of 10 mCi was used. The absorbers were prepared by a mixture of sample material (<1 mg) and thermoplastic resin, which was shaped to ca. 1-mm sized cylinders under mild heating (<100 °C), placed on strip tape and positioned close to the source. The spectra were collected at room-temperature over the velocity range -4.2 to $+4.2$ mm^{-1} distributed over 1024 channels and were calibrated against an α -Fe foil before folding and spectral fitting using the software MossA [49].

3. Microbial Clay Mineralization

Several studies emphasize the importance of microbial cells in the precipitation of iron rich minerals, in particular authigenic clays [1–5,7,22,50,51]. Studies focused on prokaryotic mineralization show that biogenic clay authigenesis occurs through a two-step process, where the initial encrustation of iron surrounding cells or filaments is followed by a secondary step of Al-Si complexation [7]. This process can result in the formation of amorphous aluminosilicate phases surrounding the microbial cell wall or EPS. Microorganisms can thus become completely or partly mineralized, with the newly formed clay grains tangentially attached to the cell wall [7]. An early cellularly bound iron-phase seems to act as a ligand that initiates subsequent precipitation of poorly crystallized aluminosilicates, potentially in the form of a precursor gel, which eventually mature into more crystalline clay phases, with the potential for fossil record preservation [13–19,25,32,52,53].

While clay formation may occur as a result of abiotic processes, for example chemical weathering resulting from interaction between oxygenated seawater and reducing basaltic rock, or hydrothermal water circulation [54], the presence of microbial cells and the biofilm EPS, appear to play a significant role in clay authigenesis [1–3,7,51–53]. One way to differentiate between biotically precipitated clay phases and those formed by abiotic processes, is to compare the degree of heterogeneity and crystallinity within the clay phases [7]. For example, Si has been proposed to play a larger role in the structure of abiotic clays, compared to biogenic bacterial precipitates, which are characterized by a lower Si concentration, smaller grain size, and frequently a more amorphous structure [7]. Further, the ratio of various elements within the clays has a large impact on the physical stability and geochemical characteristics of the mineral [55]. In smectites, for example, the amount of structural Fe affects the swelling ability of the clay phase; and Fe-rich smectites have a reduced expansion ability compared with lower Fe smectites [56]. The association and interaction between microbes and clay-forming elements described above appears to occur in many types of environments. For example, Sanchez-Navaz et al. [52] described the mineralization of iron-rich, poorly ordered and amorphous smectites in association with apatite grains within phosphatic stromatolites from the Upper Jurassic. They suggest that the presence of authigenic smectites in microbially produced stromatolite lamina are the result of a biogenically produced precursor-phase rich in Fe-Si-Al, which matures into a smectite phase during early diagenesis [52]. Here, the presence of the microbial biofilm EPS presumably acts as a catalyst for the attraction of cations and other chemical species forming the precursor gel-like phase, which subsequently develops into a clay like aluminosilicates [52]. Further, in oligotrophic granite at the Äspö hard rock laboratory near Oskarshamn in Sweden, experiments were initiated where microorganisms from Äspö were isolated and cultured within water from the area [57]. The results showed significant precipitation of minute-sized clay particles within the presence of microbial communities, and in contrast, controlled experiments without microorganisms showed no precipitation of aluminosilicate phases [57]. Results from this experiment, therefore, suggested that either the metabolic activity, or the active surface of biological cells and matrices, were important components for the precipitation of authigenic clay phases.

Wierzbos et al. [24] similarly reported bacterial sheaths and potential fungal hyphae surrounded by Fe-rich aluminosilicate phases, in cracks or fissures within Antarctic rocks. They suggested that the combination of filaments covered in an Fe-oxyhydroxide layer and associated lamina of clay-like material, could be used as a biosignature in other similar type of settings [24]. According to the authors, it was also possible to distinguish between clays associated with well-preserved filamentous microfossils, and those of more taphonomically altered specimens; the clays surrounding dead and lysed cells tended to have a larger Fe-concentration, and in turn less Si and Al present within the clay matrix. The opposite relationship could be established among exceptionally preserved specimens [24].

Further, Fe-rich minerals close in composition to Nontronite, the Fe³⁺-rich endmember of the smectite group, formed around microbial cells and their EPS within pillow lavas from the North East Pacific Ocean [50]. The smectite-covered communities were found in the vicinity of hydrothermal vents, which could have provided a source for Fe and Mn, which were observed in the form of oxides in association to biogenic clays. It could be established by Transmission Electron Microscopy (TEM) that the smectite phases were clearly growing from the cell walls of bacteria [50], again confirming the importance of the reactive cell surface to the nucleation and subsequent precipitation of clay-like minerals.

Similarly, within submerged laboratory cultures, Fomina and Gadd [20] examined the effect of clay on the formation of fungal pellets. Their results showed a significant thickening and lengthening of the fungal hyphae as a result of micro-sized clay particles that attached to the filaments from their suspension in the surrounding water. The absorption of clay particles onto hyphae affected the geochemical properties and permeability of the fungal pellets as well as added physical stability and strength [20].

As mentioned in the above section, the presence of an active cell surface or organic matrix like EPS, seem to play a ubiquitous part in the initial nucleation and precipitation of amorphous clay phases: The intimate relationship between microbial EPS and authigenic clays among both prokaryotes and eukaryotes is presumably due to the natural effect of microbial biofilms to attract and bind cations from the ambient fluids onto negatively charged functional groups [46,47,58–60]. Microbial EPS have often been highlighted as important agents in mineral precipitation. This has been especially noted in relation to the precipitation of calcite [44,45,47,59,61], which can precipitate within the EPS either as a result of the metabolic activity of cells, or simply by acting as a cation-trap and nucleation spot associated with acidic functional groups [45]. Important to note, however, is the dual role of EPS in mineral precipitation; because of the adsorptive properties of the organic substances, an initial inhibition of nucleation is to be expected, which is only surpassed once the cation binding-capacity of the biofilm EPS has been reached [45–47]. It is, therefore, easy to imagine a similar scenario with respect to for example Fe (e.g., [1–3,7]), in settings less supersaturated with calcite, that might instead lead to the formation of an amorphous clay-like phase in association with the EPS, depending on the ambient source of metals. Hence, extrinsic factors, such as element-availability, alkalinity, pH and saturation state of ambient fluids are all parameters that may have an effect on the type of mineralization that occurs [47].

Although a majority of studies have focused on the mineral promoting effect of prokaryotic biofilms [1–4,7], many fungal communities likewise produce large amounts of EPS, with similar cation-attracting characteristics [62–65]. Most fungi that produce EPS are aerobic, or possibly facultative anaerobs [62], and fungal production of EPS can be stimulated by increased pO₂ [65]. Ueshima and Tazaki [63], for example, showed a connection between fungal EPS and the formation of Fe-rich clay phases in the form of nontronite, which formed within the EPS, again highlighting the connection between microbes and EPS, but this time among heterotrophic eukaryotes.

One of the most important extrinsic factors that may have an effect on the production of fungal biofilm EPS, and thus in turn for clay precipitation, is the ambient pH of the host solution and growth medium [64,66]. For example, variations in pH can influence the molecular weight, as well as yield, of fungal EPS [66]. It appears as though an acidic pH generally promotes EPS production among

fungi [66], and, in turn, gives a lower EPS yield, but with a higher molecular weight, compared to high pH settings that promote a low molecular weight but high EPS yield [66]. This means that the ambient environment is expected to have a large influence on fungal EPS production in general, but also on the type of mineralization that will occur. Thus, for fungal clay authigenesis, pH and EPS yield may be locally important and variable factors.

3.1. Benefits of Clay Authigenesis for Microbial Communities

Although a close spatial relationship between microbial cells, filaments and more or less well-crystallized clay phases, has been established repeatedly and from a variety of settings, the exact reason for, or nature of, the relationship between microbes and clay is still not entirely clear. While it may simply be the result of geochemical processes associated with the specific structure of active microbial surfaces, several studies suggest it may in fact be beneficial for microbial communities to surround the cells and EPS with clay phases as a way to modify the ambient surroundings favorably [67]. Because clays, like microbial exopolymers, are characterized by the capacity to attract and exchange a multitude of nutrients and chemical species, this may indicate that the clay phases serve as a proximal nutrient-source for the communities [7]. This may be particularly important in extreme settings such as the highly oligotrophic igneous crust. Swelling smectite minerals such as montmorillonite, could help to stabilize the microenvironment with respect to pH, which may act beneficial on parameters such as microbial growth and respiration [7,68]. The clay can also form a protective matrix to guard viable cells against harmful effects of the surroundings, such as toxic species or damaging UV radiation [7,11,69–73]. Even many metals such as Na, K, Cu, Zn, Co, Ca, Mg, Mn, Fe, which can be considered bio-essential for fungal growth in lower concentrations, may become inhibiting in larger concentrations and can be bioremediated by means of fungal activity [20,21,69,70,74]. Within the laboratory environment, it has also been noted that clay mineralization induced by fungal pellets in suspension, may have diffusive effects on oxygen and nutrient uptake-exchange within the pellets, and that the clay particles can act as a barrier to remove toxic compounds [20].

3.2. Clays as Biosignatures

Iron is an omnipresent component of many, if not most, clays [75]. This is presumably a result of its great abundance in Earth's crust [75]. The valency and internal ratio of Fe^{2+} to Fe^{3+} within clay structures have a significant effect on the physiochemical properties of clays, such as their ability to expand, cation-exchange capacity (CEC) and surface area (e.g., [56,76]), meaning that variations in clay mineralogy may be linked to the redox capacity of the precipitating fluids. Because of the element-complexing properties found within the clay structure, clay minerals are known to form complexes with many different chemical species, including organic molecules [77–79]. This may be partly attributed to the interconnection between clays and iron, including Fe oxides, which has a special affinity to complex organic molecules that prevent the prevalent oxidation of organics [80,81]. Therefore, the suggested stepwise accretion of Fe onto microbial cells followed by subsequent attraction and complexation of Al and Si [7] may be responsible for the high organic content of clays. Since clays thus can act as a protective barrier of organics, this may be a relevant reason to focus on iron rich clays or reactive Fe-species when it comes to the search for biomarkers in sedimentary deposits on Earth or possibly on Mars [81,82].

A majority of studies concerning microbial clay authigenesis have focused on prokaryote communities in more or less shallow sedimentary environments. There is, however, a glaring gap in the knowledge of microbial clay authigenesis within the igneous crust of continents and ocean, which together represents some of the world's largest microbial habitats [83]. The oceanic crust can also provide an analogous setting for a potential subsurface-biosphere on Mars and understanding microbial preservation in cryptic seafloor habitats on Earth may thus help us to better recognize similar processes on other planets. Therefore, the following sections will more specifically focus on mineralization of clays within the subsurface igneous crust, primarily but not exclusively, among fossil

fungi. We will try to summarize the type of clay minerals that are primarily associated with biofilms in these types of extreme settings.

4. Microbial Clay Mineralization in the Igneous Crust: 2.4 Ga–48 Ma

4.1. Clay Fossilized Filaments from the Ongeluk Formation, South Africa

Ophiolitic pillow basalts from the Paleoproterozoic (2.4. Ga) Ongeluk formation, Griquatown West Basin, South Africa, was investigated by Bengtson et al. [19], who described filamentous fossils from secondary infilled amygdales in the basalt (Figure 1A–D). The Ongeluk basalt is estimated to have undergone low grade-type metamorphism, and the chlorite-mineralized filaments show metamorphic temperatures of 179–260 °C [19]. Individual filaments vary in size between 2–12 µm, but each filament has a consistent width throughout the length (Figure 1D). The filaments form intricate mycelium-like networks with morphological characteristics that suggest a fungal-like affinity (Figure 1D), which makes the Ongeluk fossils the currently oldest known fungus-like organisms in the fossil record, with large implications for the divergence of early opisthokonts [19].

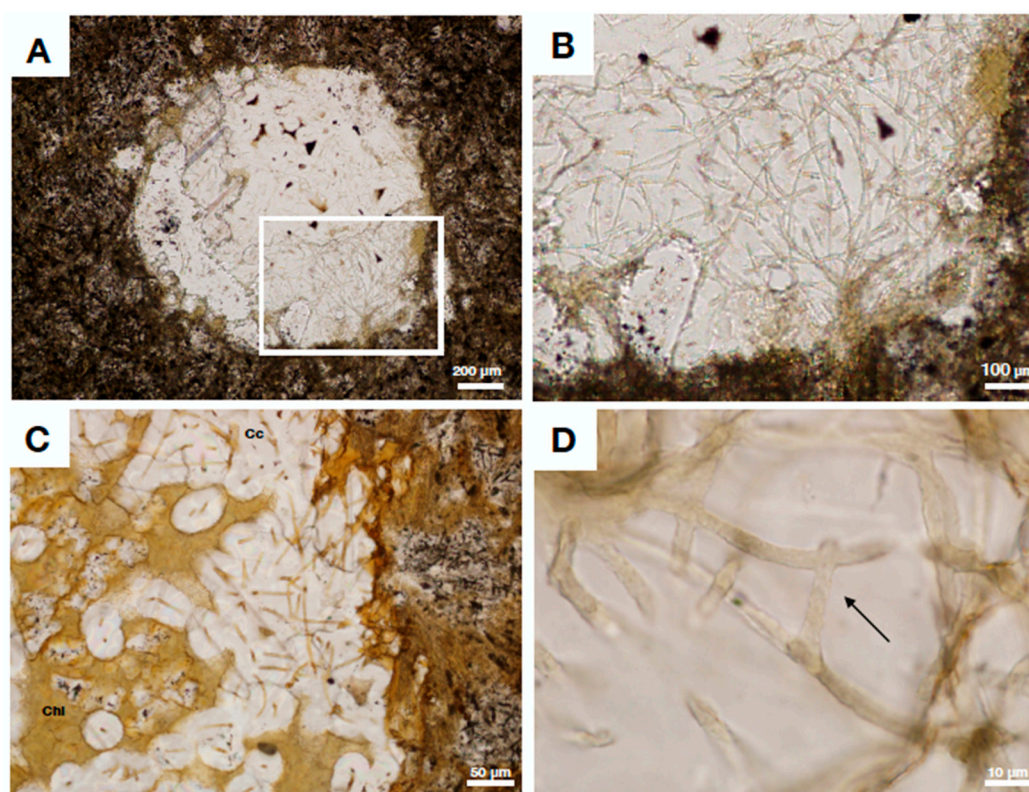


Figure 1. Optical micrographs of basalt from the Ongeluk formation, South Africa, showing a vesicle with extensive fungal-like mycelia consisting of chlorite. (A) Vesicle in basalt matrix with fungal chloritized hyphae surrounded by secondary infilled calcite. Boxed area is enlarged in (B). Scale bar equals 200 µm (B) Enlarged area from (A) showing dense fungal-like mycelia protruding from the walls into a vesicle. Filaments consist of chlorite and are enclosed in calcite. Scale bar is 100 µm. (C) Detail of chloritic fungal hyphae surrounded by calcite. Chlorite is yellow, calcite white. Scale bar equals 50 µm. (D) Chlorite filaments with even diameters show fungal like characteristics such as potential anastomosis (arrow). Scale bar equals 10 µm.

SEM-EDS analysis from the study showed that the chloritized filaments have elemental compositions corresponding to the basal fossil biofilms, from which they extend [19], suggesting a similar biological origin of both filaments and biofilm. All examined samples have matrices composed of chlorite, quartz, feldspar and calcite, with apatite and Fe-Ti oxides as main accessory minerals [19].

The metamorphic nature of the chloritized filaments made it difficult to identify the composition of the original clay phases of the Ongeluk filaments; a potential precursor mineral might have been a smectite such as saponite, or berthierine from the chlorine-group [84]. A secondary chlorite phase in the Ongeluk samples is associated with chalcopyrite and were thus presumably affected by a higher-degree metamorphism with subsequent circulation of hydrothermal fluids (i.e., [19]). Due to the endolithic characteristics of the fossils, the microorganisms must have entered the basalt during the time-window where the cooling cracks and vug-system of the basalt was still open to sea-water circulation [19], but prior to the closure of the system by secondary mineralizations. A conservative age estimate of the filaments was therefore 2.06 Ga; after the termination of fluid circulation within the rocks and closing of the amygdalae [19]. By 2.06 Ga, the deep oceans were presumably largely anoxic [85], which would imply that the Ongeluk biota had a largely anaerobic lifestyle.

4.2. Fungal Fossils from Fractured Granitic Rock

Drake et al. [25] described the first known occurrence of presumed anaerobic fossil fungi from a cored borehole within fractured granitic rock from the Laxemar-site, near the Äspö research laboratory, in Sweden. The samples described in the study are from a sectioned core taken at 740 m depth, where fossil filamentous microbes show distinctive mycelia-like characteristics (Figure 2A–F). Due to difficulties of constraining the timing of colonization, as well as the age of secondary mineralizations, the exact age of the filaments remains unknown. They are however presumably of Phanerozoic age, resting in 1.8 Ga granite host rock. The filaments are preserved as partly kerogenous, and partly clay mineralized fossils (e.g., Figure 2C) and occur in open fractures that run through a quartz-vein [25]. Stable carbon isotope SIMS microanalyses showed that the calcite precipitated along the edges of the fossil-bearing crack have substantially negative isotope values, down to $\delta^{13}\text{C}$ -43‰V-PDB, indicative of anaerobic methane oxidizing metabolisms, in association to the fungal communities [25]. The fungi have diameters ranging from 2–20 μm , and both EDS and Raman spectroscopic analysis reveal that the filaments consist of clay-like Fe-Mg-Ca- phases, as well as some minor Fe oxides [25].

For this study, we looked closer at two cores from the Laxemar area: XLX09 taken at 740 m depth and XCX04 taken at 678 m depth, to identify clay mineralogy and to characterize the redox state of iron by investigating the ratio of structural $\text{Fe}^{2+}/\text{Fe}_{\text{tot}}$ within the clays (Figure 2D,E,G). The clay phase in the XLX09 core is a light beige-white substance, constricted to filamentous fungal hyphae (Figure 2D,E). The second core, XCX04, contains a more mature biofilm with less well-preserved hyphae and a darker, brown, clay phase (Figure 2G). Subsequent XRD analysis show that the main clay phase associated with the fungi from core XLX09, is a swelling smectite of dioctahedral montmorillonite-type (with some peaks also matching that of the trioctahedral smectite saponite), with a $\text{Fe}^{2+}/\text{Fe}_{\text{tot}}$ ratio of 33.9 % (Figure 3A,B). The second core (XCX04), with a darker clay phase, showed no significant swelling during a second XRD run with prepared wet-samples, however the analysed peaks were closest matched by montmorillonite, again with some peak overlap of saponite. $\text{Fe}^{2+}/\text{Fe}_{\text{tot}}$ was 30.6 %, i.e., it showed a small but significantly lower proportion of Fe^{2+} within the mineral structure compared to the white fungal clay phase in XLX09 (Figure 3A,C).

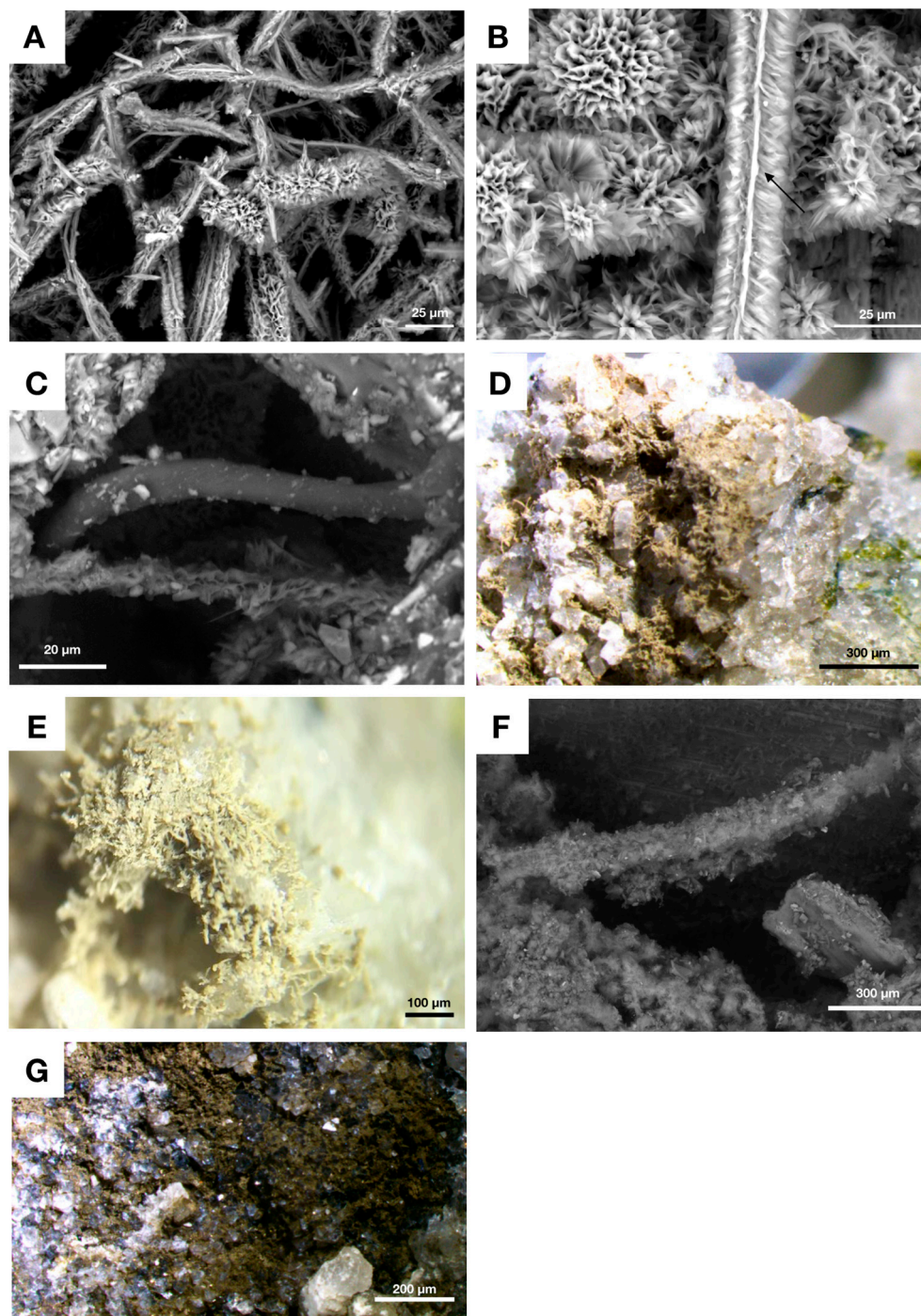


Figure 2. Scanning electron (A–C,F,G) and stereo (D,E) micrographs of fungal fossils from fractured granitic rock, Laxemar drill-cores, Sweden. The fossils are preserved mainly by clay mineralization but also as carbonaceous filaments. (A) Clay mineralized hyphae with a central strand. Scale bar equals 25 μm . (B) Close-up of clay mineralized hyphae with a central strand (arrow). Scale bar equals 25 μm . (C) Part clay-part carbonaceous fungal hyphae preserved within a hollow fracture. Scale bar equals 20 μm . (D) Sample of flight fungal biofilm from Laxemar run by XRD and Mössbauer spectroscopy for this review. Calcite surround the biofilm. Scale bar equals 300 μm . (E) Close-up of light fungal clay mineralized hyphae run by XRD and Mössbauer spectroscopy for this review. Scale bar equals 100 μm . (F) Poorly preserved fungal hyphae with uneven clay encrustation. Scale bar equals 300 μm . (G) XRD and Mössbauer spectroscopy sample showing a dark clay phase assumed to represent altered fungal biofilm from Laxemar. Scale bar equals 200 μm .

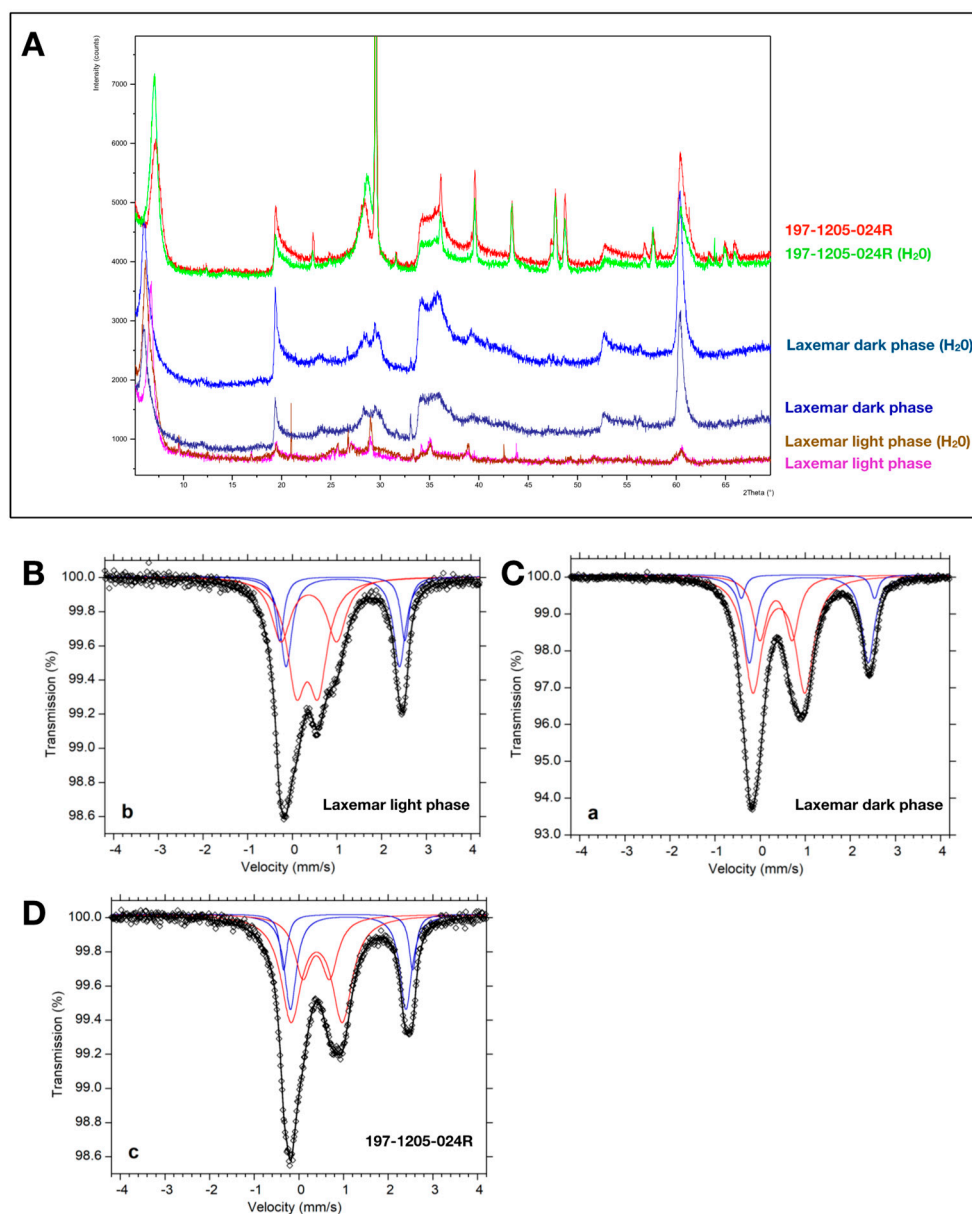


Figure 3. XRD (A) and Mössbauer spectra (B–D) of sample 1205A-024R (Nintoku seamount, clay mineralized hyphae) and two fungal biofilm samples (light and dark) from Laxemar, Sweden. (A) Summary of all XRD spectra encoded by color showing XRD peaks most closely related to smectites, in particular montmorillonite (there are also some peak matches with the smectite-group mineral saponite). (B) Mössbauer spectrum of light-colored clay mineralized fungal filaments from Laxemar. Diamonds represent the measured spectrum; the thick solid line represents the sum of the two fitted doublets (thin lines) assigned to Fe^{3+} and Fe^{2+} ($\text{Fe}^{2+}/\text{Fe}_{\text{tot}}$: 33.9%). (C) Mössbauer spectrum of slightly altered dark-colored clay mineralized biofilm from Laxemar. Diamonds represent the measured spectrum; the thick solid line represents the sum of the two fitted doublets (thin lines) assigned to Fe^{3+} and Fe^{2+} ($\text{Fe}^{2+}/\text{Fe}_{\text{tot}}$: 30.6%). (D) Mössbauer spectrum of green-colored clay mineralized fungal filaments from sample 1205A-024R, Nontoku seamount. Diamonds represent the measured spectrum; the thick solid line represents the sum of the two fitted doublets (thin lines) assigned to Fe^{3+} and Fe^{2+} ($\text{Fe}^{2+}/\text{Fe}_{\text{tot}}$: 33.5%).

4.3. Fungal Biofilms within The Emperor Seamounts

Together with Hawaii, the Emperor seamounts, a submarine volcanic chain named in large after famous Japanese Emperors, extends over 5000 km in the Pacific Ocean and contains a sequence of

volcanic islands and seamounts, presumably resulting from hotspot volcanism [25]. The chain has a north-south trend after which it bends to the south east- the oldest part, approximately 81 Ma, lies in the North East and the chain becomes successively younger until, by about 43 Ma, it bends towards the younger Hawaii islands.

Detroit seamount is situated in the northernmost, and oldest, part of the Emperor chain, and was drilled at several locations in 2001 (ODP leg197, cores 1203, 1204A and 1204B) [86]. The seamount holds pillow basalts with an age of approximately 81 Ma [35], dating back to the Cretaceous period. Within these cores, Ivarsson et al. [15,16], reported the presence of clay-fossilized fungi from a depth of 936.65 mbsf within the seamount (Figure 4A–D). The fossil fungal filaments and sporophore-like structures (e.g., Figure 4D) were closely associated with the presence of botryoidal Mn-oxides (Figure 4A–C), suggested to have a biological and possibly fungal, origin [16]. The fossil biofilms, green in stereo microscopic-reflected light, were identified in open vesicles (Figure 4A,C) and the filaments are attached to a basal biofilm, from which they protruded into the open space of the vug [16].

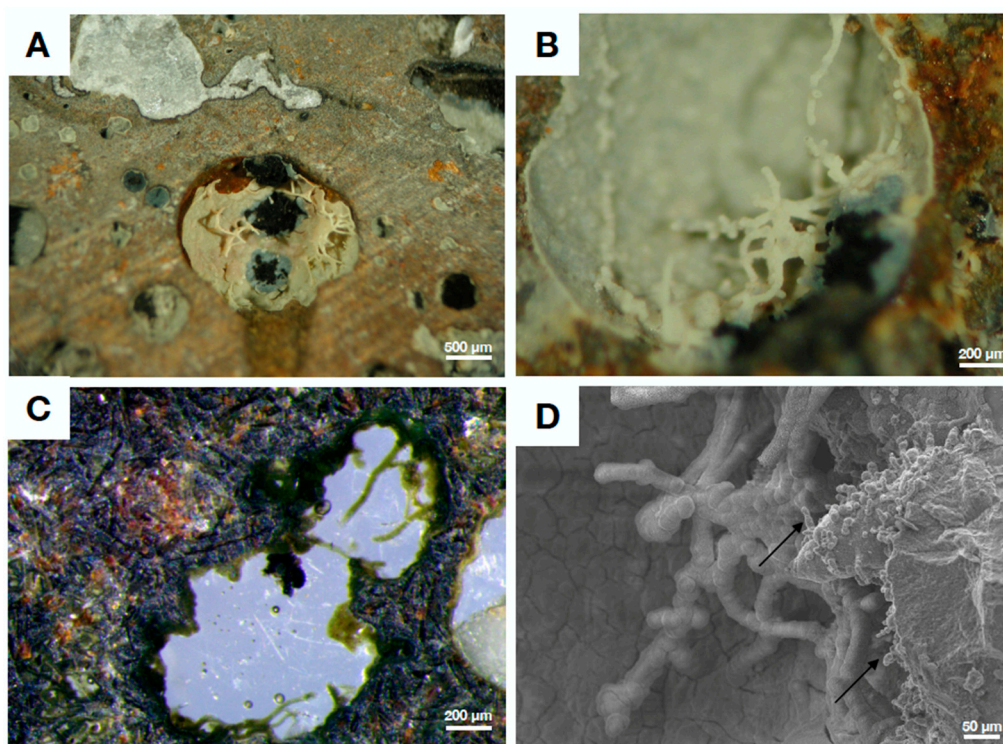


Figure 4. Stereo (A–C) and Scanning Electron micrographs of fungal biofilms protruding from the walls into empty or partly filled vesicles within basalt from Detroit seamount, samples 1204B-16R-01 and 1203A-57R3. (A) vesicle filled with authigenic clay (yellow-cream) and Mn-oxides (black). Fungal hyphae are preserved in clay within the vesicle. Scale bar equals 500 µm. (B) Close-up of hyphae and basal biofilm preserved as clay with a basalt matrix. Scale bar equals 200 µm. (C) Vesicle with green-colored clay mineralized filaments and biofilm protruding into an empty void surrounded by basalt matrix. Scale bar equals 200 µm. (D) Fungal mycelia with potential sporophore structures (arrows). Scale bar equals 50 µm.

The basal biofilm as well as the filaments have similar compositions and consist of Fe-rich smectites [16]. The smectite phases were analysed using Raman spectroscopy, and showed distinct peaks most closely corresponding to Nontronite, the Fe³⁺-rich smectite endmember. A few spectral variations however suggested the possibility of a mixed signal for the clay phases, possibly corresponding to a Ca-poor montmorillonite (e.g., see [16]).

Ivarsson et al. [17], also investigated basaltic drill core samples from the Nintoku seamount, situated centrally within the Emperor submarine chain of Paleocene/Eocene age, dated to approximately 56 Ma.

The authors examined a cored section from IODP sample site 197-1206-34R, and therein described an extensive fracture system, split open to expose fossil biofilms and associated microbial structures which had formed along the fracture-walls (Figure 5A–F). The exposed biofilm was 20–100 μm thick and contained cell-like structures comparable to yeast growth-phases (Figure 5E,F). Filamentous fungi, 15–25 μm in diameter, extended from the basal film in a complex mycelia-like fashion, comparable to that of other samples from the Emperor chain (e.g., Ivarsson et al. [15,16]. XRD and Raman spectroscopy analysis showed that both biofilm and filaments consisted of a swelling smectite-layer, most closely related to montmorillonite. In association to the hypha, cauliflower-like hematite bodies similar to microstromatolites were found, consisting of banded hematite [17].

Another IODP sample (197-1205A-024R) from Nintoku seamount was analysed using XRD and Mössbauer spectroscopy for this review in order to ascertain the clay composition and iron redox state at a different location within the seamount. The sample contained a green clay phase with a basal biofilm and filaments corresponding in morphology to fungal hyphae similar to those described by Ivarsson et al. above (Figure 5G). The hyphae consisted of a swelling smectite phase closely corresponding to XRD spectra from montmorillonite (with some peaks also matching that of saponite), with $\text{Fe}^{2+}/\text{Fe}_{\text{tot}}$ ratio of 33.5 % (Figure 3A,D). These results correspond well to the XRD results obtained by Ivarsson et al. [17] from other depths at site 1205A and suggests a consistency with respect to the main clay phases present at different locations and depths within the Nintoku seamount, but also between different seamounts within the Emperor chain as well.

One of the youngest seamounts in the Emperor chain is Koko seamount, an underwater volcano dated to the Eocene epoch at 48 Ma [35]. Koko seamount rises approximately 5000 m from the abyssal plain, and Bengtson et al. [18] described from IODP sample 197-1206A-4R filamentous mycelia-like networks consisting of hematite tubules surrounded by a montmorillonite-like clay layer that extended from partly open vugs and vesicles in the basalt (Figure 6A–D). The fossil filaments were attached to a basal biofilm, with an outer crust consisting of a montmorillonite-phase similar to those surrounding the filaments. The base of the biofilm, however, was found to consist of hematite with carbon, and an upper hematite layer and montmorillonite type clay on top [18]. The hyphae extending from the basal film were often associated with cauliflower-like iron rich microstromatolites (Figure 6D), similar to the fungal systems present in Nintoku seamount (e.g., [17]).

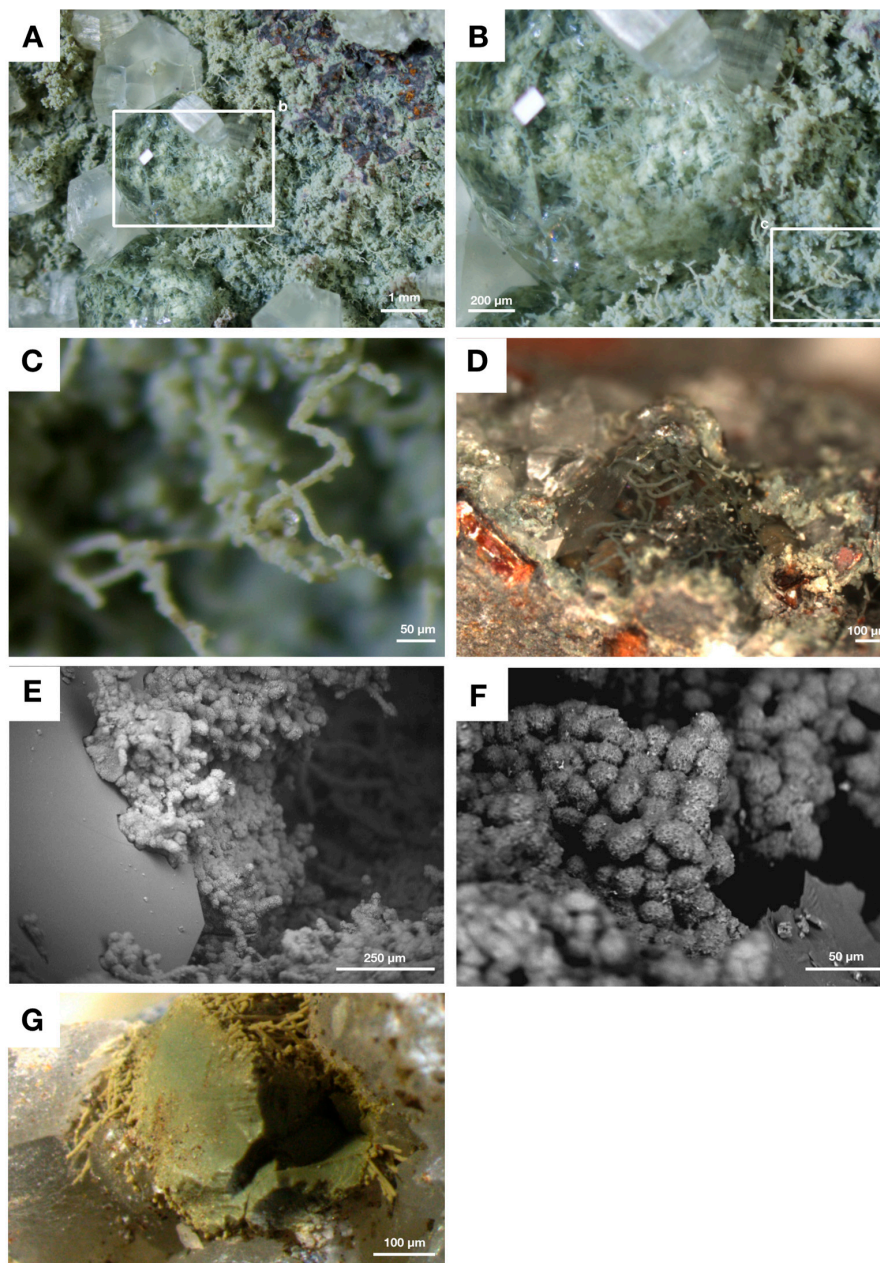


Figure 5. Stereo (A–D,G) and Scanning Electron micrographs showing fungal biofilm with yeast-like structures preserved in green clay from samples 1205-34R-5 (A–F) and 1206A-024R (G), Nintoku seamount. (A) Open fracture exposing filamentous fungal biofilms preserved in clay, partly intergrown and overgrown by zeolites (translucent minerals) with dark Mn-oxides present. Boxed area is magnified in (B). Scale bar is 1 mm. (B) Close-up of boxed area from (A) showing clay mineralized hyphae intergrown with zeolite crystal. Boxed area is magnified in (C). Scale bar is 200 µm. (C) Close-up of boxed area from (B). Evenly preserved clay mineralized fungal hyphae with spore-like structures attached. Scale bar is 50 µm. (D) Fungal mycelium intergrown with zeolites. Scale bar is 100 µm. (E) Fungal biofilm with yeast-like cells attached to the surface. Scale bar is 250 µm. (F) Close-up of yeast-like cells from fungal biofilm. All cells and hyphae are preserved as authigenic clays. Scale bar is 50 µm. (G) XRD and Mössbauer-run sample 1206A-024R, showing green clay mineralized fungal filaments. Scale bar is 100 µm.

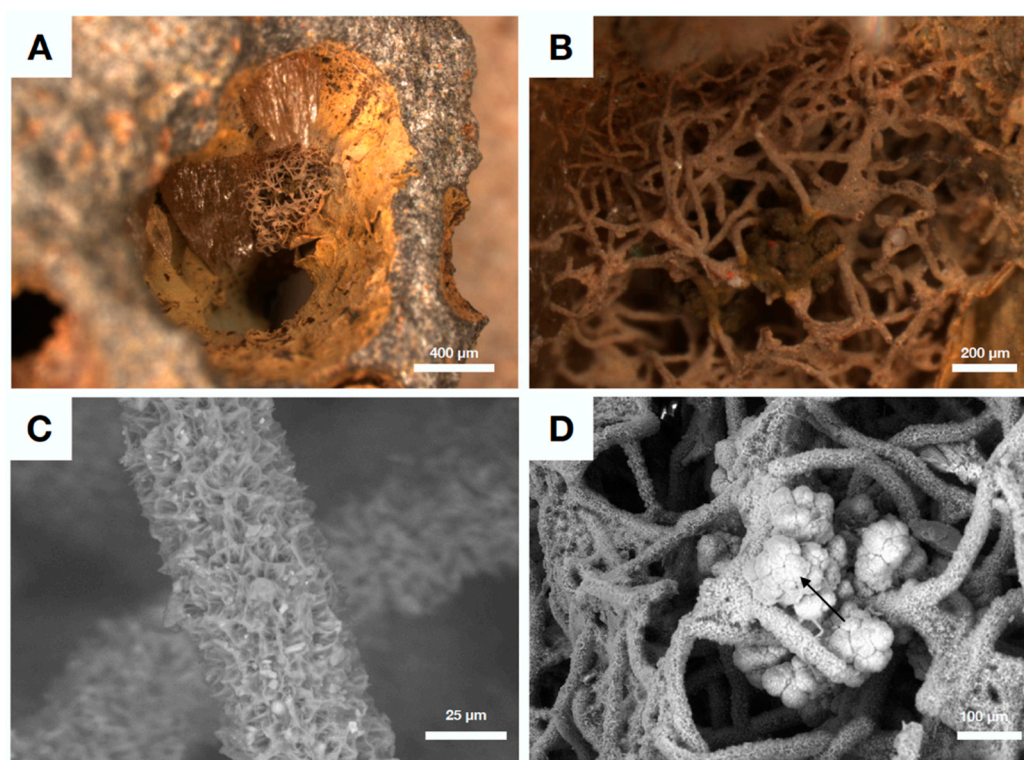


Figure 6. Stereo (A–B) and Scanning Electron micrographs (C–D) of clay mineralized fungal biofilms from Koko seamount, sample 1206-4R-2. (A) Vesicle containing clay encrusted mycelia that branch and diverge. Scale bar is 400 μm . (B) Close-up of pristine mycelia network preserved in a rust-colored clay. Scale bar is 200 μm . (C) Close-up of evenly clay encrusted fungal hyphae. Scale bar is 24 μm . (D) Fungal mycelia with embedded cauliflower-like microstromatolites of *Frutexites*-type (arrow).

4.4. Authigenic Clays within Late Devonian Pillow Basalts

Eickmann et al. [14] described the presence of fossilized cryptoendolithic filaments, of uncertain biological affinity, found in calcite-filled vesicles from ophiolitic Late Devonian pillow basalts in Germany. The filaments were preserved by clay mineralization, with an endmember composition similar to berthierine (with 36% of Fe as Fe^{2+})-chamosite/illite for the central strand, and illite-glaucanite precipitated like a halo around the central strand. The precipitation of clay as described by Eickmann et al. [14] presumably proceeded as a passive mineralization of active functional groups on filament surfaces, similar to the process described by [7]. The most pristine filaments in the study contained Chamosite, the Fe^{2+} endmember of the chlorite group, indicating that encrustation of microbial cells proceeded from a poorly ordered Fe, Al silicate phase to a more crystalline chamosite (e.g., [2,13]). Similarly, Peckmann et al. [13] described microbial clay encrustation analogous to the Fe-Si encrustation explained from many other studies of mainly prokaryote biofilms (e.g., [1–5,7] and references therein), related to cryptoendolithic filamentous microorganisms from another German ophiolitic pillow basalt. Two kind of filaments were identified in the study; the first with an illite center consisting of a thin outer chamosite rim, and the other with a central TiO_2 strand surrounded by illite with an outer rim of chamosite.

5. Redox Variability in Crustal Biosphere Habitats

Studies of microbial clay authigenesis in the igneous crust have so far only scratched the surface. However, the antiquity of for example the fungus-like Ongeluk fossils (Figure 1) described by Bengtson et al. [17], testifies to the fundamental nature of microbial clay mineralization in the deep subseafloor crust, extending as far back as the Paleoproterozoic. It is apparent from many studies i.e., [1–5,7–10,13–19,25,33–39] that authigenic mineral precipitation, in particular clay authigenesis,

related to microbial communities and their EPS seems to follow a similar pattern (see e.g., [7]) among prokaryotes as well as within most fungal biofilms. This suggests an analogous mode of formation, albeit with some variations, particularly in the style and degree of microbial preservation within the igneous crust. Variations in the orogenic history of the source rock, may be one reason for these differences. How variations in oxygen levels and thus the redox state of a system affects fungal clay authigenesis, including the type of clay that forms, is however more uncertain: Seamounts and oceanic spreading centers are commonly uncovered by sediments, and can work as oxygen pumps of sorts, circulating oxygenated seawater through the porous upper oceanic crust, i.e., [87]. Generally, within the deep ocean sediments, oxygen is rapidly used up through reactions with organic material in the shallow upper layers, which leave significant parts of deep-sea sediments essentially anoxic [87]. At the sediment-basalt interface, however, increased oxygen concentrations are to be expected due to the input of oxygen-rich oceanic water circulating within the crust and diffusing upwards, into the sediments [87]. The description of especially Fe and Mn oxides in amygdales and cracks within oceanic basalts (e.g., [16,35]) are good indications of at least partly oxygenated conditions within the oceanic crust, permitting the transportation of otherwise insoluble Fe and Mn species. However, the oceanic crust is heterogenous, and even if the oceanic crust in general is believed to be more or less oxygenated [88], locally reducing conditions may prevail in places where anoxic or sub-oxic fluids from hydrothermal sources reach the crust [87] or in areas extending away from mid-ocean ridges and hotspots.

Oxygenation within a sealed space may also be subject to variations on the temporal scale during which colonization of the basalt takes place affecting the subsequent precipitation of secondary minerals: For example, McKinley et al. [11], describe clay authigenesis in Miocene flood basalts, where fractures containing clay-fossilized filaments of presumed prokaryotic nature also contain a range of secondary minerals such as oxic ferrihydrite, trioctahedral Fe²⁺-rich smectites, pyrite and quartz, together suggesting that local conditions were initially oxic, but turned progressively anoxic [11], emphasizing the variable nature of the basaltic crust.

Our review of authigenic clay precipitation within fungal communities suggest that the impact of oxygen on the precipitating clay phase may in fact be rather negligible, at least within the deep crust, seeing as the preferred mineralogy associated with fossil fungi from both anoxic deep granite rocks as well as oxygenic seamount basalts, are similar types of swelling montmorillonites (see Table 1 for comparison of clay mineralization among various herein discussed localities). Similarities in our XRD spectra with that of the trioctahedral smectite saponite is also worth to mention, seeing as saponite clay have been attributed to the activity of microbial communities in hydrothermal settings from Iceland, recently described by Geptner et al. [53]. Various members of the chlorite group have been more sporadically described associated with deep biosphere microbial fossils, i.e., [13,14,19], all with ages ranging from Devonian or older. Also, the degree of structural Fe²⁺ is roughly equal between these settings, with a small but significant difference of about 2.9% more Fe²⁺ within montmorillonites/smectites precipitated under anoxic conditions.

Table 1. Summary of studies focusing on subsurface clay authigenesis associated with (mainly) fungal biofilms. Publications are arranged according to age from the top-down.

Reference	Age	Setting	Preservation	Clay Phase	Color of Clay	Assumed Source Fluid (This Review)
[19]	Bedrock 2.4 Ga (filament ages ~2.06 Ga)	Ongeluk ophiolite, South Africa	Clay mineralization, slightly metamorphic and chloritized	Chlorite (transformed from precursor clay)	Pale yellow-brown	Anoxic
[25]	Bedrock 1.8 Ga (filament ages not constrained, Phanerozoic)	Continental fractured granite Laxemar, Sweden (drill cores)	Clay mineralization/carbonaceous filaments	Fe/Mg/Ca-rich clay, minor Fe-oxides	Cream white (sample XLX09)	Anoxic
[13]	Presumed Devonian	Arnstein ophiolite, Germany (pillow basalt)	Clay mineralization	TiO ₂ filament-strands surrounded by illite and chamosite	Pale yellow-brown	Presumed oxic-sub oxic
[14]	Presumed Devonian	Frankenwald and Thüringer Wald, Germany (pillow basalt)	Clay mineralization	Illite center/chamosite rim or TiO ₂ filament-strands surrounded by illite and chamosite	Green	Presumed oxic-sub oxic
[16]	Cretaceous, 81 Ma	Oceanic crust, Detroit seamount (basalt drill cores)	Clay mineralization	Smectite (montmorillonite)	Cream yellow (sample 197-1204B-16R-01)	Oxic -slightly sub oxic
[17]	Paleocene-Eocene boundary, 56 Ma	Oceanic crust, Nintoku seamount (basalt drill cores)	Clay mineralization	Smectite (montmorillonite)	Green (sample 197-1205-34R-5)	Oxic -slightly sub oxic
[15]	Paleocene-Eocene boundary, 56 Ma (Nintoku seamount)/ Eocene, 48 Ma (Koko seamount)	Oceanic crust, Nintoku and Koko seamounts (basalt drill cores)	Clay mineralization	Smectite (montmorillonite)	Green (sample 197-1205-34R-5), Yellow-cream/red (sample 197-1206-4R-2)	Oxic -slightly sub oxic
[18]	Eocene, 48 Ma	Oceanic crust, Koko seamount (basalt drill cores)	Clay mineralization	Smectite (montmorillonite)	Yellow-cream/red (sample 197-1206-4R-2)	Oxic -slightly sub oxic

Noteworthy is that the preservation of filamentous fungi from the Pacific Ocean Emperor seamounts appears to have occurred *in vivo*, or possibly very early *post mortem*, considering the pristine nature of the clay-encrusted filaments (i.e., Figures 4–6). The mycelia are evenly encrusted and structurally intact, forming complex 3D networks (i.e., Figure 6). They do not appear collapsed, and filaments can rather often be seen protruding in or out of associated secondary minerals such as zeolites (Figure 5A–D). All filaments described by Ivarsson et al. and Bengtson et al. from the Emperor seamounts [15–19,33–38], are thus encrusted by mainly smectites in the form of montmorillonite-type clays. Swelling smectites such as montmorillonite in particular, are particularly sensitive to alteration processes that can affect the structure and mineralogy of the clay, i.e., [89]. Smectites are also among the most prone to destabilization due to for example microbial iron reduction [90], which make smectites including montmorillonite-type clays good indicators of fairly juvenile, or unaltered, conditions within sealed vesicles or cracks. These characteristics of smectites corresponds well to the structural fidelity of the montmorillonite-encrusted fungi from especially the Emperor seamounts. Intriguingly, the fungi preserved by clay mineralization in the anoxic deep crust, exemplified here by the Laxemar fungal fossils (Figure 2), appear less well-preserved, compared with the pristine fossils of basaltic seamounts (i.e., compare Figure 2C,F to Figures 5 and 6). In a few cases, it is possible to observe that the Laxemar filaments are only partly encrusted with montmorillonite clays and the remainder of the filament is instead preserved as kerogenous fossils (Figure 2C). In all, mineralization in these settings appear to have been less continuous, and this together with the irregularity of preserved specimens, might suggest that mineralization did not occur while the organisms were alive, but rather as a post mortem process on top of carbonaceous filaments. Thus, the presence of oxygen in the ambient environment appears to have a small effect on the type of clay mineral that forms. However, the effect of oxygen may be larger when it comes to the timing and mode of fossil preservation, especially related to the preservation of kerogenous filaments, which may be more pronounced in low oxygen settings.

One potential driving mechanism behind the structural differences exhibited by montmorillonite-covered fungi in anoxic granitic versus oxic basaltic settings, may be related to the production and structure of fungal EPS, which can differ greatly between oxygen-variable settings; In general, fungal EPS production is stimulated by the presence of oxygen and can be lower or absent among anaerobic fungi [62]. Fungal EPS, like microbial EPS in general, is expected to play a significant part in the mineralization process, acting as a cation-trap and potential mineral nucleation-source, eventually promoting further mineral precipitation [45]. Therefore, the amount as well as the structure of the fungal EPS may well affect the degree and style of mineralization within fungal communities as well.

Looking closer at some of the ophiolitic settings described by Bengtson et al. [19], Peckmann et al. [13] and Eickmann et al. [14], the taphonomy of microbial preservation here seems rather similar; with filaments preserved as a central strand surrounded first by a halo and then by an outer rim, with different mineral compositions. This may suggest that various physical and diagenetic processes related to the uplift of oceanic crust onto continents have affected both the mineralogy and taphonomy of the cryptoendolithic microbes. The abundance of chlorite mineral members from all of these locations support such a theory, seeing as chlorite derived from various precursor clay minerals are common processes during low temperature (<200 °C) alterations (e.g., [84]). The complex nature of preservation, with several different mineral phases or “zones”, may thus be the result of a complex diagenetic and orogenic history, compared to microbial fossils containing only one juvenile clay phase, such as smectites of montmorillonite-type (see e.g., [89]).

Further supporting a more complex mode of microfossil-preservation in relation to low temperature alterations, are microfossil-finds by Sakakibara et al. [91] within pre-Jurassic age metabasaltic rocks from central Shikoku, Japan. This study described the presence of branching filamentous microbes within previously water-filled vesicles within the basalt, which allowed the formation of microbial clay within the open space, thus preserving the putative microorganisms. In the case of the Sakakibara [91] fossils, these are preserved as central filamentous strands composed of Fe oxides and surrounded by

a halo of phengite with a rim of pumpellyite—all of which could have formed from microbial clay precursors such as illite-glaucanite (for phengite) and illite-chamosite (for pumpellyite) during light metamorphism [91].

6. Summary

Preservation of cryptoendolithic microbial communities, especially fungi, within Earth's igneous crust is intimately linked to the precipitation of authigenic clays. In particular swelling smectite minerals such as montmorillonite, have been described from various deep subsurface localities. Our study suggests a larger input from biology on the formation of clays in the subsurface igneous crust of both land and oceans, than what has hitherto been recognized. While traditionally, the external environment has been suggested to control the mineralogy of precipitating clays to a large extent, our results suggest that similar type of swelling smectites form associated with fungal filaments and biofilms in subsurface crustal settings highly variable with respect to both source rock (felsic granite versus basic basalt) and ambient pO_2 . The effect of oxygen on fungal clay precipitation, however, is likely complex, and may affect the timing as well as the taphonomy of the mineralized microbe. Overall, we suggest that intrinsic factors, such as the extracellular organic matrix, have a large impact on the type of clay that precipitates around microbial cells and EPS. This, in turn, suggests that the presence of life in the deep oligotrophic crust probably have a far greater effect on the cycling of chemical species, such as Fe, Al and Si than what has been previously established and may in fact be responsible for a great fraction of secondary clay minerals in the deep subsurface biosphere.

Author Contributions: T.S. designed and implemented the study, wrote the initial manuscript and aided with sample analysis. M.I. contributed with manuscript conception and providing samples. H.D. contributed with manuscript conception, C isotope data used in the review and providing samples. H.S. contributed with XRD, Mössbauer analysis and manuscript conception.

Funding: This research was funded by a Carl Trygger Foundation post-doctoral grant (CTS 18:167) to TS and MI, a Swedish Research Council grant (contracts No. 2012-4364, 2017-04129) to MI, a Villum Investigator grant to Donald Canfield (No. 16518), a Swedish Research Council grant (contract 2017-05186) and a Formas grant (contract 2017-00766) to HD.

Acknowledgments: The authors wish to thank the Swedish Nuclear Fuel and Waste Management Co (SKB) for access to drill core samples.

Conflicts of Interest: The authors declare no conflict of interest.

References

1. Ferris, F.G.; Beveridge, T.J.; Fyfe, W.S. Iron-silica crystallite nucleation by bacteria in a geothermal sediment. *Nature* **1986**, *320*, 609–611. [[CrossRef](#)]
2. Ferris, F.; Fyfe, W.; Beveridge, T. Bacteria as nucleation sites for authigenic minerals in a metal-contaminated lake sediment. *Chem. Geol.* **1987**, *63*, 225–232. [[CrossRef](#)]
3. Ferris, F.G.; Fyfe, W.S.; Beveridge, T.J. Bacteria as nucleation sites for authigenic minerals. In *Developments in Geochemistry*; Elsevier: Amsterdam, The Netherlands, 1991; Volume 6, pp. 319–325.
4. Konhauser, K.O.; Fyfe, W.S.; Ferris, F.G.; Beveridge, T.J. Metal sorption and mineral precipitation by bacteria in two Amazonian river systems: Rio Solimões and Rio Negro, Brazil. *Geology* **1993**, *21*, 1103–1106. [[CrossRef](#)]
5. Konhauser, K.O.; Schultze-Lam, S.; Ferris, F.G.; Fyfe, W.S.; Longstaffe, F.J.; Beveridge, T.J. Mineral Precipitation by Epilithic Biofilms in the Speed River, Ontario, Canada. *Appl. Environ. Microbiol.* **1994**, *60*, 549–553. [[PubMed](#)]
6. Chafetz, H.S.; Buczynski, C. Bacterially induced lithification of microbial mats. *Palaios* **1992**, *7*, 277–293. [[CrossRef](#)]
7. Konhauser, K.O.; Urrutia, M.M. Bacterial clay authigenesis: a common biogeochemical process. *Chem. Geol.* **1999**, *161*, 399–413. [[CrossRef](#)]
8. Knorre, H.V.; Krumbein, W.E. Bacterial calcification. In *Microbial Sediments*; Springer: Berlin/Heidelberg, Germany, 2000; pp. 25–31.

9. Konhauser, K.O.; Hamade, T.; Raiswell, R.; Morris, R.C.; Ferris, F.G.; Southam, G.; Canfield, D.E. Could bacteria have formed the Precambrian banded iron formations? *Geology* **2002**, *30*, 1079–1082. [[CrossRef](#)]
10. Vasconcelos, C.; Warthmann, R.; McKenzie, J.A.; Visscher, P.T.; Bittermann, A.G.; van Lith, Y. Lithifying microbial mats in Lagoa Vermelha, Brazil: modern Precambrian relics? *Sediment. Geol.* **2006**, *185*, 175–183. [[CrossRef](#)]
11. McKinley, J.P.; Stevens, T.O.; Westall, F. Microfossils and paleoenvironments in deep subsurface basalt samples. *Geomicrobiol. J.* **2000**, *17*, 43–54.
12. Schiffman, P.; Fisher, Q.J.; Konhauser, K.O. Microbial mediation of authigenic clays during hydrothermal alteration of basaltic tephra, Kilauea Volcano. *Geochem. Geophys. Geosystems* **2002**, *3*, 1–13.
13. Peckmann, J.; Bach, W.; Behrens, K.; Reitner, J. Putative cryptoendolithic life in Devonian pillow basalt, Rheinisches Schiefergebirge, Germany. *Geobiology* **2008**, *6*, 125–135. [[CrossRef](#)]
14. Eickmann, B.; Bach, W.; Kiel, S.; Reitner, J.; Peckmann, J. Evidence for cryptoendolithic life in Devonian pillow basalts of Variscan orogens, Germany. *Palaeogeogr. Palaeoclim. Palaeoecol.* **2009**, *283*, 120–125. [[CrossRef](#)]
15. Ivarsson, M.; Bengtson, S.; Skogby, H.; Belivanova, V.; Marone, F. Fungal colonies in open fractures of subseafloor basalt. *Geo-Marine Lett.* **2013**, *33*, 233–243. [[CrossRef](#)]
16. Ivarsson, M.; Broman, C.; Gustafsson, H.; Holm, N.G. Biogenic Mn-oxides in subseafloor basalts. *PLoS ONE* **2015**, *10*. [[CrossRef](#)]
17. Ivarsson, M.; Bengtson, S.; Skogby, H.; Lazor, P.; Broman, C.; Belivanova, V.; Marone, F. A fungal-prokaryotic consortium at the basalt-zeolite interface in subseafloor igneous crust. *PLoS ONE* **2015**, *10*. [[CrossRef](#)]
18. Bengtson, S.; Ivarsson, M.; Astolfo, A.; Belivanova, V.; Broman, C.; Marone, F.; Stampanoni, M. Deep-biosphere consortium of fungi and prokaryotes in Eocene subseafloor basalts. *Geobiology* **2014**, *12*, 489–496. [[CrossRef](#)]
19. Bengtson, S.; Rasmussen, B.; Ivarsson, M.; Muhling, J.; Broman, C.; Marone, F.; Stampanoni, M.; Bekker, A. Fungus-like mycelial fossils in 2.4-billion-year-old vesicular basalt. *Nat. Ecol. Evol.* **2017**, *1*, 141. [[CrossRef](#)]
20. Fomina, M.; Gadd, G.M. Influence of clay minerals on the morphology of fungal pellets. *Mycol. Res.* **2002**, *106*, 107–117. [[CrossRef](#)]
21. Fomina, M.; Gadd, G.M. Metal sorption by biomass of melanin-producing fungi grown in clay containing medium. *J. Chem. Technol. Biotechnol.* **2003**, *78*, 23–34. [[CrossRef](#)]
22. Konhauser, K.O. Diversity of bacterial iron mineralization. *Earth-Science Rev.* **1998**, *43*, 91–121. [[CrossRef](#)]
23. Konhauser, K.O.; Ferris, F.G. Diversity of iron and silica precipitation by microbial mats in hydrothermal waters, Iceland: Implications for Precambrian iron formations. *Geology* **1996**, *24*, 323. [[CrossRef](#)]
24. Wierzchos, J.; Ascaso, C.; Sancho, L.G.; Green, A. Iron-Rich Diagenetic Minerals are Biomarkers of Microbial Activity in Antarctic Rocks. *Geomicrobiol. J.* **2003**, *20*, 15–24. [[CrossRef](#)]
25. Drake, H.; Ivarsson, M.; Bengtson, S.; Heim, C.; Siljeström, S.; Whitehouse, M.J.; Broman, C.; Belivanova, V.; Åström, M.E. Anaerobic consortia of fungi and sulfate reducing bacteria in deep granite fractures. *Nat. Commun.* **2017**, *8*, 55. [[CrossRef](#)]
26. Edwards, K.J.; Rogers, D.R.; Wirsén, C.O.; McCollom, T.M. Isolation and characterization of novel psychrophilic, neutrophilic, Fe-oxidizing, chemolithoautotrophic α - and γ -Proteobacteria from the Deep Sea. *Appl. Environ. Microbiol.* **2003**, *69*, 2906–2913. [[CrossRef](#)]
27. Edwards, K.J.; Fisher, A.T.; Wheat, C.G. The Deep Subsurface Biosphere in Igneous Ocean Crust: Frontier Habitats for Microbiological Exploration. *Front. Microbiol.* **2012**, *3*, 8. [[CrossRef](#)]
28. Orcutt, B.N.; Sylvan, J.B.; Knab, N.J.; Edwards, K.J. Microbial ecology of the Dark Ocean above, at, and below the seafloor. *Microbiol. Mol. Biol. Rev.* **2011**, *75*, 361–422. [[CrossRef](#)]
29. Thorseth, I.; Torsvik, T.; Furnes, H.; Muehlenbachs, K. Microbes play an important role in the alteration of oceanic crust. *Chem. Geol.* **1995**, *126*, 137–146. [[CrossRef](#)]
30. Staudigel, H.; Furnes, H.; McLoughlin, N.; Banerjee, N.R.; Connell, L.B.; Templeton, A. 3.5 billion years of glass bioalteration: Volcanic rocks as a basis for microbial life? *Earth-Sci. Rev.* **2008**, *89*, 156–176. [[CrossRef](#)]
31. Banerjee, N.R.; Izawa, M.R.M.; Sapers, H.M.; Whitehouse, M.J. Geochemical biosignatures preserved in microbially altered basaltic glass. *Surf. Interface Anal.* **2011**, *43*, 452–457. [[CrossRef](#)]
32. Schumann, G.; Manz, W.; Reitner, J.; Lustrino, M. Ancient fungal life in North Pacific Eocene oceanic crust. *Geomicrobiol. J.* **2004**, *21*, 241–246. [[CrossRef](#)]
33. Ivarsson, M.; Lindblom, S.; Broman, C.; Holm, N.G. Fossilized microorganisms associated with zeolite–carbonate interfaces in sub-seafloor hydrothermal environments. *Geobiology* **2008**, *6*, 155–170. [[CrossRef](#)]

34. Ivarsson, M.; Lausmaa, J.; Lindblom, S.; Broman, C.; Holm, N.G. Fossilized microorganisms from the Emperor Seamounts: Implications for the search for a subsurface fossil record on Earth and Mars. *Astrobiology* **2008**, *8*, 1139–1157. [[CrossRef](#)]
35. Ivarsson, M.; Bengtson, S.; Belivanova, V.; Stampanoni, M.; Marone, F.; Tehler, A. Fossilized fungi in subseafloor Eocene basalts. *Geology* **2012**, *40*, 163–166. [[CrossRef](#)]
36. Ivarsson, M.; Holm, N.G.; Neubeck, A. The deep biosphere of the subseafloor igneous crust. In *Trace Metal Biogeochemistry and Ecology of Deep-Sea Hydrothermal Vent Systems*; Demina, L.L., Galkin, S.V., Eds.; Springer: Cham, Switzerland, 2015; pp. 1–24.
37. Ivarsson, M.; Schnürer, A.; Bengtson, S.; Neubeck, A. Anaerobic Fungi: A Potential Source of Biological H₂ in the Oceanic Crust. *Front. Microbiol.* **2016**, *7*, 674. [[CrossRef](#)]
38. Ivarsson, M.; Bengtson, S.; Neubeck, A. The igneous oceanic crust – Earth’s largest fungal habitat? *Fungal Ecol.* **2016**, *20*, 249–255. [[CrossRef](#)]
39. Drake, H.; Ivarsson, M.; Tillberg, M.; Whitehouse, M.; Kooijman, E. Ancient microbial activity in deep hydraulically conductive fracture zones within the forsmark target area for geological nuclear waste disposal, Sweden. *Geosciences* **2018**, *8*, 211. [[CrossRef](#)]
40. Drake, H.; Ivarsson, M. The role of anaerobic fungi in fundamental biogeochemical cycles in the deep biosphere. *Fungal Boil. Rev.* **2018**, *32*, 20–25. [[CrossRef](#)]
41. Sutherland, I.W. Biofilm exopolysaccharides: a strong and sticky framework. *Microbiol.* **2001**, *147*, 3–9. [[CrossRef](#)]
42. Flemming, H.C.; Neu, T.R.; Wozniak, D.J. The EPS matrix: the “house of biofilm cells”. *J. Bacteriol.* **2007**, *189*, 7945–7947. [[CrossRef](#)]
43. Costerton, J.W.; Lewandowski, Z.; Caldwell, D.E.; Korber, D.R.; Lappin-Scott, H.M. Microbial biofilms. *Annu. Rev. Microbiol.* **1995**, *49*, 711–745. [[CrossRef](#)]
44. Arp, G.; Reimer, A.; Reitner, J. Calcification in cyanobacterial biofilms of alkaline salt lakes. *Eur. J. Phycol.* **1999**, *34*, 393–403. [[CrossRef](#)]
45. Arp, G. Photosynthesis-Induced Biofilm Calcification and Calcium Concentrations in Phanerozoic Oceans. *Science* **2001**, *292*, 1701–1704. [[CrossRef](#)]
46. Dupraz, C.; Visscher, P.T. Microbial lithification in marine stromatolites and hypersaline mats. *Trends Microbiol.* **2005**, *13*, 429–438. [[CrossRef](#)]
47. Dupraz, C.; Reid, R.P.; Braissant, O.; Decho, A.W.; Norman, R.S.; Visscher, P.T. Processes of carbonate precipitation in modern microbial mats. *Earth-Science Rev.* **2009**, *96*, 141–162. [[CrossRef](#)]
48. Hazen, R.M.; Schiffrins, C.M. Why deep carbon? *Rev. Mineral. Geochem.* **2013**, *75*, 1–6. [[CrossRef](#)]
49. Prescher, C.; McCammon, C.; Dubrovinsky, L. MossA: A program for analyzing energy-domain Mössbauer spectra from conventional and synchrotron sources. *J. Appl. Crystallogr.* **2012**, *45*, 329–331. [[CrossRef](#)]
50. Fortin, D.; Ferris, F.G.; Scott, S.D. Formation of Fe-silicates and Fe-oxides on bacterial surfaces in samples collected near hydrothermal vents on the Southern Explorer Ridge in the Northeast Pacific Ocean. *Am. Miner.* **1998**, *83*, 1399–1408. [[CrossRef](#)]
51. Léveillé, R.J.; Datta, S. Lava tubes and basaltic caves as astrobiological targets on Earth and Mars: A review. *Planet. Space Sci.* **2010**, *58*, 592–598. [[CrossRef](#)]
52. Sánchez- Navas, A.S.; Algarra, A.M. Nieto Bacterially-mediated authigenesis of clays in phosphate stromatolites. *Sedimentology* **1998**, *45*, 519–533. [[CrossRef](#)]
53. Geptner, A.; Kristmannsdóttir, H.; Kristjánsson, J.; Marteinson, V. Biogenic Saponite from an Active Submarine Hot Spring, Iceland. *Clays Clay Miner.* **2002**, *50*, 174–185. [[CrossRef](#)]
54. Bristow, T.F.; Milliken, R.E. Terrestrial perspective on authigenic clay mineral production in ancient Martian lakes. *Clays Clay Miner.* **2011**, *59*, 339–358. [[CrossRef](#)]
55. Stumm, W.; Morgan, J.J. *Aquatic Chemistry An Introduction Emphasizing Chemical Equilibria in Natural Waters*; John Wiley & Sons: New York, NY, USA, 1981.
56. Stucki, J.W. Structural iron in smectites. In *Iron in Soils and Clay Minerals*; Springer: Dordrecht, The Netherlands, 1988; pp. 625–675.
57. Tuck, V.A.; Edyvean, R.G.J.; West, J.M.; Bateman, K.; Coombs, P.; Milodowski, A.E.; McKervey, J.A. Biologically induced clay formation in subsurface granitic environments. *J. Geochem. Explor.* **2006**, *90*, 123–133. [[CrossRef](#)]
58. Castanier, S.; Le Metayer-Levrel, G.; Perthuisot, J.P. Bacterial roles in the precipitation of carbonate minerals. In *Microbial Sediments*; Springer: Berlin/Heidelberg, Germany, 2000; pp. 32–39.

59. Braissant, O.; Decho, A.W.; Przekop, K.M.; Gallagher, K.L.; Glunk, C.; Dupraz, C.; Visscher, P.T. Characteristics and turnover of exopolymeric substances in a hypersaline microbial mat. *FEMS Microbiol. Ecol.* **2009**, *67*, 293–307. [[CrossRef](#)]
60. Dupraz, C.; Fowler, A.; Tobias, C.; Visscher, P.T. Stromatolitic knobs in Storr's Lake (San Salvador, Bahamas): A model system for formation and alteration of laminae. *Geobiology* **2013**, *11*, 527–548. [[CrossRef](#)]
61. Arp, G.; Thiel, V.; Reimer, A.; Michaelis, W.; Reitner, J. Biofilm exopolymers control microbialite formation at thermal springs discharging into the alkaline Pyramid Lake, Nevada, USA. *Sediment. Geol.* **1999**, *126*, 159–176. [[CrossRef](#)]
62. Sandford, P.A. Exocellular, microbial polysaccharides. In *Advances in Carbohydrate Chemistry and Biochemistry*; Academic Press: Cambridge, MA, USA, 1979; Volume 36, pp. 265–313.
63. Ueshima, M.; Tazaki, K. Possible role of microbial polysaccharides in nontronite formation. *Clays Clay Miner.* **2001**, *49*, 292–299. [[CrossRef](#)]
64. Abdel-Aziz, M.S.; Hamed, H.A.; Mouafi, F.E.; Gad, A.S. Acidic pH-shock induces the production of an exopolysaccharide by the fungus *Mucor rouxii*: Utilization of beet-molasses. *NY Sci. J.* **2012**, *5*, 52–61.
65. Mahapatra, S.; Banerjee, D. Fungal Exopolysaccharide: Production, Composition and Applications. *Microbiol. Insights* **2013**, *6*, 1–16. [[CrossRef](#)]
66. Wang, Y.; McNeil, B. Production of the fungal exopolysaccharide scleroglucan by cultivation of *Sclerotium gluconicum* in an airlift reactor with an external loop. *J. Chem. Technol. Biotechnol.* **1995**, *63*, 215–222. [[CrossRef](#)]
67. England, L.S.; Lee, H.; Trevors, J.T. Bacterial survival in soil: Effect of clays and protozoa. *Soil Biol. Biochem.* **1993**, *25*, 525–531. [[CrossRef](#)]
68. Stotzky, G.; Rem, L.T. Influence of clay minerals on microorganisms: I. Montmorillonite and kaolinite on bacteria. *Can. J. Microbiol.* **1966**, *12*, 547–563. [[CrossRef](#)]
69. Morley, G.F.; Gadd, G.M. Sorption of toxic metals by fungi and clay minerals. *Mycol. Res.* **1995**, *99*, 1429–1438. [[CrossRef](#)]
70. Gadd, G.M. Interactions of fungi with toxic metals. In *The Genus Aspergillus*; Springer: Boston, MA, USA, 1994; pp. 361–374.
71. Blaudez, D.; Jacob, C.; Turnau, K.; Colpaert, J.V.; Ahonen-Jonnarth, U.; Finlay, R.; Botton, B.; Chalot, M. Differential responses of ectomycorrhizal fungi to heavy metals in vitro. *Mycol. Res.* **2000**, *104*, 1366–1371. [[CrossRef](#)]
72. Perotto, S.; Martino, E. Molecular and cellular mechanisms of heavy metal tolerance in mycorrhizal fungi: What perspectives for bioremediation? *Min. Biotechnol.* **2001**, *13*, 55–63.
73. Baldrián, P. Interactions of heavy metals with white-rot fungi. *Enzym. Microb. Technol.* **2003**, *32*, 78–91. [[CrossRef](#)]
74. Gadd, G.M. Geomycology: biogeochemical transformations of rocks, minerals, metals and radionuclides by fungi, bioweathering and bioremediation. *Mycol. Res.* **2007**, *111*, 3–49. [[CrossRef](#)]
75. Stucki, J.W. Properties and behaviour of iron in clay minerals. *Dev. Clay Sci.* **2006**, *1*, 423–475.
76. Zhu, R.; Chen, Q.; Zhou, Q.; Xi, Y.; Zhu, J.; He, H. Adsorbents based on montmorillonite for contaminant removal from water: A review. *Appl. Clay Sci.* **2016**, *123*, 239–258. [[CrossRef](#)]
77. Yu, G.H.; He, P.J.; Shao, L.M. Characteristics of extracellular polymeric substances (EPS) fractions from excess sludges and their effects on biofloculability. *Bioresour. Technol.* **2009**, *100*, 3193–3198. [[CrossRef](#)]
78. Kennedy, M.J.; Löhr, S.C.; Fraser, S.A.; Baruch, E.T. Direct evidence for organic carbon preservation as clay-organic nanocomposites in a Devonian black shale; from deposition to diagenesis. *Earth Planet. Sci. Lett.* **2014**, *388*, 59–70. [[CrossRef](#)]
79. Playter, T.; Konhauser, K.; Owttrim, G.; Hodgson, C.; Warchola, T.; Mloszewska, A.M.; Sutherland, B.; Bekker, A.; Zonneveld, J.-P.; Pemberton, S.G.; et al. Microbe-clay interactions as a mechanism for the preservation of organic matter and trace metal biosignatures in black shales. *Chem. Geol.* **2017**, *459*, 75–90. [[CrossRef](#)]
80. LaLonde, K.; Mucci, A.; Ouellet, A.; Gelinás, Y. Preservation of organic matter in sediments promoted by iron. *Nature* **2012**, *483*, 198–200. [[CrossRef](#)]
81. Parenteau, M.N.; Jahnke, L.L.; Farmer, J.D.; Cady, S.L. Production and Early Preservation of Lipid Biomarkers in Iron Hot Springs. *Astrobiology* **2014**, *14*, 502–521. [[CrossRef](#)]

82. Summons, R.E.; Amend, J.P.; Bish, D.; Buick, R.; Cody, G.D.; Marais, D.J.D.; Dromart, G.; Eigenbrode, J.L.; Knoll, A.H.; Sumner, D.Y. Preservation of Martian Organic and Environmental Records: Final Report of the Mars Biosignature Working Group. *Astrobiology* **2011**, *11*, 157–181. [[CrossRef](#)]
83. Magnabosco, C.; Lin, L.-H.; Dong, H.; Bomberg, M.; Ghiorse, W.; Stan-Lotter, H.; Pedersen, K.; Kieft, T.L.; Van Heerden, E.; Onstott, T.C. The biomass and biodiversity of the continental subsurface. *Nat. Geosci.* **2018**, *11*, 707. [[CrossRef](#)]
84. Beaufort, D.; Rigault, C.; Billon, S.; Billault, V.; Inoue, A.; Inoue, S.; Patrier, P. Chlorite and chloritization processes through mixed-layer mineral series in low-temperature geological systems—a review. *Clay Miner.* **2015**, *50*, 497–523. [[CrossRef](#)]
85. Canfield, D.E. A new model for Proterozoic ocean chemistry. *Nature* **1998**, *396*, 450–453. [[CrossRef](#)]
86. Tarduno, J.A.; Duncan, R.A.; Scholl, D.W. *Leg 197 Summary: Proceedings of the Ocean Drilling Program, Initial Reports*; Ocean Drilling Program Texas A&M University: College Station TX, USA, 2002; Volume 197, pp. 1–92.
87. Orcutt, B.N.; Wheat, C.G.; Rouxel, O.; Hulme, S.; Edwards, K.J.; Bach, W. Oxygen consumption rates in subsurface basaltic crust derived from a reaction transport model. *Nat. Commun.* **2013**, *4*, 2539. [[CrossRef](#)]
88. Bach, W.; Edwards, K.J. Iron and sulfide oxidation within the basaltic ocean crust: implications for chemolithoautotrophic microbial biomass production. *Geochim. Cosmochim. Acta* **2003**, *67*, 3871–3887. [[CrossRef](#)]
89. Tosca, N.J.; Knoll, A.H. Juvenile chemical sediments and the long term persistence of water at the surface of Mars. *Earth Planet. Sci. Lett.* **2009**, *286*, 379–386. [[CrossRef](#)]
90. Dong, H.; Jaisi, D.P.; Kim, J.; Zhang, G. Microbe-clay mineral interactions. *Am. Mineral.* **2009**, *94*, 1505–1519. [[CrossRef](#)]
91. Sakakibara, M.; Sugawara, H.; Tsuji, T.; Ikehara, M. Filamentous microbial fossil from low-grade metamorphosed basalt in northern Chichibu belt, central Shikoku, Japan. *Planet. Space Sci.* **2014**, *95*, 84–93. [[CrossRef](#)]



© 2019 by the authors. Licensee MDPI, Basel, Switzerland. This article is an open access article distributed under the terms and conditions of the Creative Commons Attribution (CC BY) license (<http://creativecommons.org/licenses/by/4.0/>).